CHAPTER 1

Introduction to photovoltaic technology and theoretical background of Perovskite Solar Cells

This Page is intentionally left blank.

Introduction

In our contemporary, technology-driven world, energy stands as a vital and irreplaceable necessity in our daily lives. The challenges of balancing energy production with the ever-increasing demands of a growing global population, urbanization, and technological progress are significant. Globally, our energy consumption is heavily dependent on various sources, with fossil fuels such as petroleum, coal, and natural gas constituting a significant 86.4% of the total energy supply [1]. This heavy reliance on fossil fuels results in the emission of harmful pollutants and greenhouse gases, leading to severe environmental damage. While nuclear power offers a large-scale energy alternative, it poses serious safety risks and complex waste management problems. To fully replace fossil fuels with nuclear energy, we must abandon the unrealistic task of constructing one 1GW nuclear fission plant daily for the next 50 years [2]. There is a potential for the clandestine extraction of weapons-grade materials from these facilities, which could contribute to the development of weapons of mass destruction. This issue raises substantial worldwide security concerns, which must be addressed. Among all renewable energy sources, solar energy stands out for its abundance, accessibility, and minimal environmental impact. Solar cells are fundamental to harnessing solar energy, converting sunlight directly into electrical power. The Earth receives an astounding amount of solar energy each year – roughly 10,000 times our current global consumption [3]. Harnessing even a fraction of this energy by covering just 0.1% of the Earth's surface with solar cells of 10% efficiency could meet our present energy needs [3]. The challenge lies in developing the technologies necessary for efficient solar energy conversion, storage, and distribution.

The Sun's energy originates from thermonuclear fusion reactions at its core, which produce a broad spectrum of electromagnetic radiation. While the entire solar spectrum ranges from 250 to 2500 nm, the visible light we perceive falls within 400 to 700 nm [4]. Interestingly, the densest portion of this visible spectrum, ideal for solar energy conversion, lies between 400 and 550 nm, offering energy densities of 1.5 to 1.75 W/m^2 per nanometer [5]. India's geographical location makes it a prime candidate for harnessing solar power. India receives substantial solar radiation daily, ranging from 4 to 7 kilowatt-hours (kWh) per square meter. When we consider this annually, it amounts

to an astonishing 5,000 trillion kWh, surpassing our current energy consumption by a significant margin.

1.1 Solar Cell Technologies

The key to harnessing the Sun's power lies in the solar cell. This ingenious device, a type of semiconductor, directly converts sunlight into electricity. Multiple solar cells are combined to form solar panels, the mainstays behind photovoltaic (PV) electricity generation. Solar cells operate cleanly, producing no harmful emissions during energy conversion, making solar energy a sustainable alternative. However, the advantages of solar power go beyond its abundance. Solar cells offer compelling environmental and economic benefits, making them stand out as a clean and sustainable alternative to traditional energy sources. The primary advantages of solar cells include their minimal maintenance requirements, ability to operate independently off-grid—suitable for remote areas or self-sustaining applications—and their complete absence of noise pollution, making them perfect for use in noise-sensitive environments. Currently, crystalline silicon modules, encompassing monocrystalline and large-grain polycrystalline silicon belonging to the "first-generation solar cells," dominate the market for around 85% of photovoltaic production as per studies [6].

Although silicon-based solar cells have been widely used, their production is still costly and energy-intensive, involving the use of high temperatures and high-vacuum techniques [7]. This led to the ‘second generation' of thin-film solar cells, which offer lower costs but reduced efficiency compared to silicon-based technology. Additionally, their widespread adoption remains restricted due to the use of scarce (like indium) or toxic (like cadmium) elements [8]. The PV landscape is rapidly changing. A new wave of 'third-generation' technologies is emerging, including dye-sensitized solar cells (DSSCs), organic photovoltaics (OPVs), and the most promising new entrant, perovskite solar cells. These benefits offer the potential to build low-cost fabrication methods that use easily available materials [9]. Let's thoroughly examine and analyze these captivating technologies.

Crystalline semiconductors have unique energy bands: a low-energy valence band where electrons typically reside and a higher-energy conduction band where they can move freely. Doping the semiconductor with specific impurities fundamentally alters

this structure. Doping with n-type material adds electrons as donors, making extra electrons readily available, while p-type doping introduces acceptors, creating vacancies known as "holes." When these differently doped materials come together, a p-n junction forms. Electrons from the n-type side naturally diffuse toward the p-type side, filling some holes. This leaves behind a region of positive charge on the n-side and negative charge on the p-side near the junction, establishing a built-in electric field. This field acts like a one-way gate within a solar cell. When sunlight strikes the solar cell, photons carrying sufficient energy displace electrons from the valence band, causing them to move into the conduction band. After that, the electric field moves the charged electrons to the n-type side and the holes to the p-type side. This coordinated charge separation drives the electric current, flowing from the n-type to the p-type side through an external wire, generating useful power. Fig 1.1 displays the discussed charge carrier movement inside the semiconductor materials.

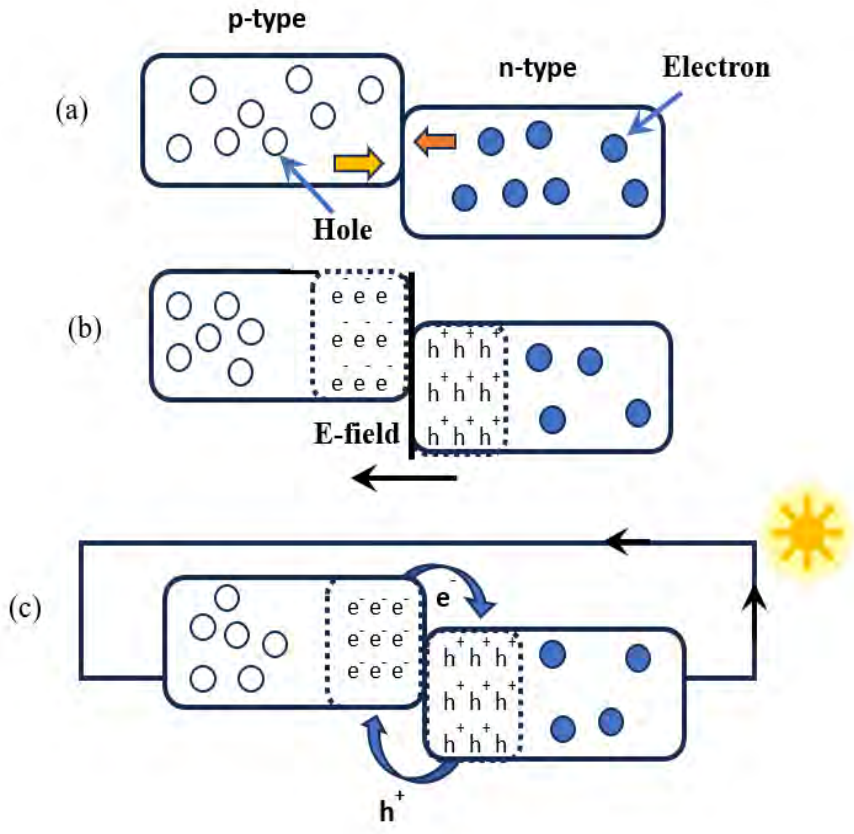

Figure 1. 1 The Band images of n-type and p-type semiconductors (a) before and (b) after joining resulting in a p-n junction. (c) Schematic of a classical sandwich solar cell composed of p- and n-type semiconductors under illumination.

1.2 Photovoltaic Generation

Photovoltaic (PV) cells offer a unique way to generate electricity by directly harnessing the power of solar energy. Their environmentally friendly operation and the sheer abundance of sunlight make solar cells an increasingly attractive energy solution. Based on their structure, materials, and performance, PV technologies can be broadly divided into three categories [10], as visualized in Figure 1.2.

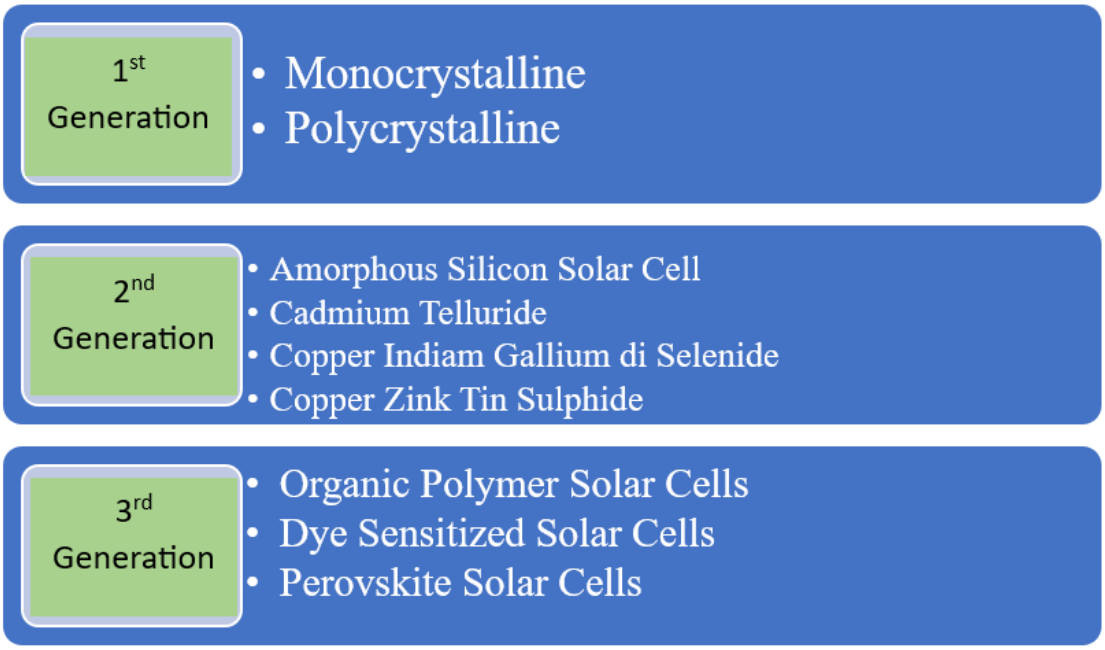

Figure 1. 2 Classification of Solar Cells

1.2.1 1st generation: Crystalline Silicon (Poly-silicon or mono-silicon) solar cells

First-generation solar cells, built primarily from high-purity silicon wafers, lead the market in efficiency. However, their dependency on highly refined materials results in high production costs. As of 2024, the highest confirmed efficiency for pure silicon-based solar cells has reached 26.81% [11]. Despite being widely used, silicon is not ideal for photovoltaic conversion due to its low optical absorption coefficient as an indirect bandgap semiconductor. To effectively capture the majority of incident light, thicker silicon layers are required, resulting in increased production costs. Consequently, while silicon-based first-generation photovoltaics are reliable, their cost-cutting option is limited. Additionally, silicon solar cell efficiencies are constrained by the theoretical Shockley-Queisser limit [12]. To overcome these issues, researchers focus on two key goals: lowering solar cell production costs and surpassing the

theoretical Shockley-Queisser limit for efficiency. The first approach focuses on developing thin-film solar cells, known as second-generation photovoltaics, while third-generation PV technologies aim to overcome the Shockley-Queisser limit.

1.2.2 2nd generation: Thin-film Solar Cell (TFSC)

Second-generation solar cells rely on thin-film technology. These films are dramatically thinner than first-generation silicon cells, measuring less than 1 μm. They're deposited on substrates like glass, metal, or plastic using various techniques. This thinness is crucial because thin-film materials have much higher absorption coefficients than silicon due to their direct bandgap. While offering a lower-cost alternative, these cells, like their predecessors, still face a theoretical maximum efficiency limit due to their single p-n junction design. In addition, thin-film technology offers benefits in the production process. Unlike individual crystalline silicon cells, thin films can easily form on larger surfaces, enabling streamlined mass production. The most common thin-film materials include amorphous silicon, micro-crystalline silicon, polycrystalline silicon, copper indium selenide, and cadmium telluride.

Amorphous silicon (a-Si) holds a significant position among second-generation thin-film materials. It's ideal for multi-junction solar cells, where layers with different bandgaps work together to capture a wider range of sunlight efficiently. Since a-Si cells are ideal for low-power applications and remarkably cheaper to produce, they offer a cost-effective solution. They use just 1% of the silicon needed for traditional cells, slashing manufacturing costs. Typically, these solar modules offer efficiencies between 4-8%. However, a-Si has a key limitation – its low quantum efficiency, meaning it collects fewer charge carriers per incoming photon. This is primarily due to the disordered structure of amorphous silicon, which leads to dangling bonds. These defects can disrupt conductivity within the material. Researchers have tackled the efficiency problem by developing tandem and triple-layer devices, stacking p-i-n cells to improve light absorption [13]. Despite these advancements, the efficiency of a-Si solar cells remains lower than their crystalline counterparts. Beyond amorphous silicon, other thin-film materials offer exciting possibilities.

Cadmium Telluride (CdTe): This material demonstrates performance comparable to crystalline silicon, coupled with the additional benefits of effectively absorbing diffuse

light and maintaining stability even under elevated temperatures [14]. CdTe holds the record for the most cost-effective thin-film technology, even surpassing crystalline silicon in some markets [15]. A wide range of manufacturing processes make CdTe suitable for large-scale production. However, using cadmium and tellurium, which are rare and toxic elements, raises environmental concerns and thus limits its widespread adoption.

Copper Indium Selenide (CIS) and Copper Indium Gallium Selenide (CIGS): Both CIS and CIGS are known for their exceptional long-term stability, making them ideal for building integrated photovoltaic applications [16]. CIGS, in particular, shines with a high light absorption coefficient, allowing it to capture a substantial amount of light even in thin films. CIGS cells exhibit an extended lifespan with minimal performance degradation, distinguishing them from other thin-film alternatives. They hold the highest certified laboratory efficiency (23.35%) and a module efficiency record of 19.64% [17, 18-20]. The combination of low fabrication costs and high efficiency makes CIGS a strong contender for the future of thin-film solar cells. Furthermore, thin-film technology offers the advantage of integrating solar panels onto flexible materials such as textiles, thereby enabling innovative applications [21-23]. While CIS and CIGS-based cells outperform polysilicon at the cell level, their module efficiency is still lower. In addition, the production of these cells involves high-temperature deposition techniques, which can be complex and costly. CIGS contains elements like indium and gallium, which are relatively rare and can have environmental and health implications.

Thin-film technology, while showing great promise, still faces several challenges. A critical challenge arises from the fact that the impressive efficiencies achieved in small-scale laboratory devices do not always seamlessly translate to large-scale modules. Furthermore, the dependence on toxic compounds like cadmium and rare elements like tellurium and indium creates significant environmental concerns. The use of hazardous materials directly contradicts the eco-friendly image of solar technology, making it a highly controversial issue.

1.2.3 3rd generation Solar Cells

Third-generation solar cells represent a significant advancement, aiming to surpass the Shockley-Queisser efficiency limit that constrains conventional designs. These cells

utilize innovative materials like organic polymers, conductive molecules, and dyes, focusing on low-cost fabrication techniques that don't rely on the high temperatures required for silicon production. A key difference in third-generation cells is the withdrawal from the basic p-n junction structure. Instead, they use multilayer designs optimized for efficient charge exchange. Organic and polymeric materials offer several advantages for solar cells, including lightweight design, flexibility, potential for low-cost production, and efficient use of materials. Specific research areas within this generation attracting significant attention include extremely thin absorber (ETA) cells, organic heterojunction solar cells, hybrid solar cells, dye-sensitized solar cells, and perovskite solar cells (PSC).

Organic Heterojunction Solar Cells consist of n-type donor materials (like polyphenylene vinylene derivatives and poly-alkyl thiophene) and p-type acceptor materials (often fullerene and its derivatives). While further advances are needed, the highest efficiency achieved for this type of cell stands at around 5.15% [24]. Extremely Thin Absorber (ETA) Solar Cells prioritize maximizing solar energy conversion efficiency. A thin, light-absorbing semiconductor layer is sandwiched between two transparent, interpenetrated nanomaterial layers designed for efficient electron and hole transport. Common choices include TiO_2 and ZnO for electron conduction and CuSCN for hole conduction [25-27]. Hybrid solar cells utilize the distinct benefits of both inorganic and organic components by combining the two. Conjugated polymers, commonly used organic materials, play a dual role: absorbing light and transporting holes (positive charges). Inorganic materials, primarily metal oxides, handle electron conduction. Combining these materials in a heterojunction (layered) structure has achieved efficiencies exceeding 5% [28].

Dye-sensitized Solar Cells (DSSCs): A breakthrough in 1991, DSSCs revolutionized the field with their innovative design inspired by photosynthesis. These cells, efficient at 7.9% energy conversion, utilize a highly porous titanium dioxide (TiO_2) film coated with dye molecules that capture sunlight, similar to chlorophyll in plants [29]. This light-sensitive layer is sandwiched between a liquid electrolyte and a platinum counter electrode. The discovery of DSSCs opened a new avenue for photovoltaic research due to their low-cost, abundant materials and simple fabrication process, often called "artificial photosynthesis" [30, 31].

Beyond traditional liquid electrolytes, researchers are exploring alternatives like gel electrolytes, ionic liquids, and polymerized hole conductors [32-37]. Over the past three decades, relentless efforts within the research community have yielded significant progress. Notably, advancements in semiconductor oxides, sensitizer molecules, electrolytes, and counter-electrode materials have contributed to the enhanced efficiency and stability of Dye-Sensitized Solar Cells (DSSCs). While DSSCs offer the advantages of low-cost manufacturing and flexibility, their efficiency, stability, and durability still lag behind those of traditional non-organic solar cells. The quest for even higher efficiency has driven the development of promising alternatives to DSSCs. Solid-state DSSCs, quantum dot-sensitized cells, and particularly perovskite solar cells (PSCs) have emerged with great interest. During the past decade, PSCs have witnessed a rapid rise in efficiency, reaching a remarkable 26.1% [38-43]. Their affordability and light-harvesting properties are outstanding, making them a strong contender in the photovoltaic race. However, challenges related to stability and lead toxicity persist, prompting active research to develop more stable and lead-free formulations for perovskite solar cells worldwide.

In conclusion, the field of solar cell technology is a testament to continuous innovation. Each generation builds upon the strengths of the last, addressing limitations and pushing the boundaries of efficiency. This relentless pursuit holds immense potential for a future powered by clean and sustainable energy sources. Collaborative efforts by researchers worldwide provide a glimpse into a future where highly efficient, environmentally friendly solar technologies become commonplace, empowering applications such as powering remote communities and revolutionizing building-integrated photovoltaics.

1.3 PEROVSKITE SOLAR CELLS

1.3.1 Introduction to Perovskite material

Perovskite solar cells have ignited the photovoltaic field with their astonishingly rapid rise in efficiency (Fig 1.3). This unprecedented leap in performance has captivated researchers worldwide, sparking an intense focus on understanding and further optimizing this promising technology.

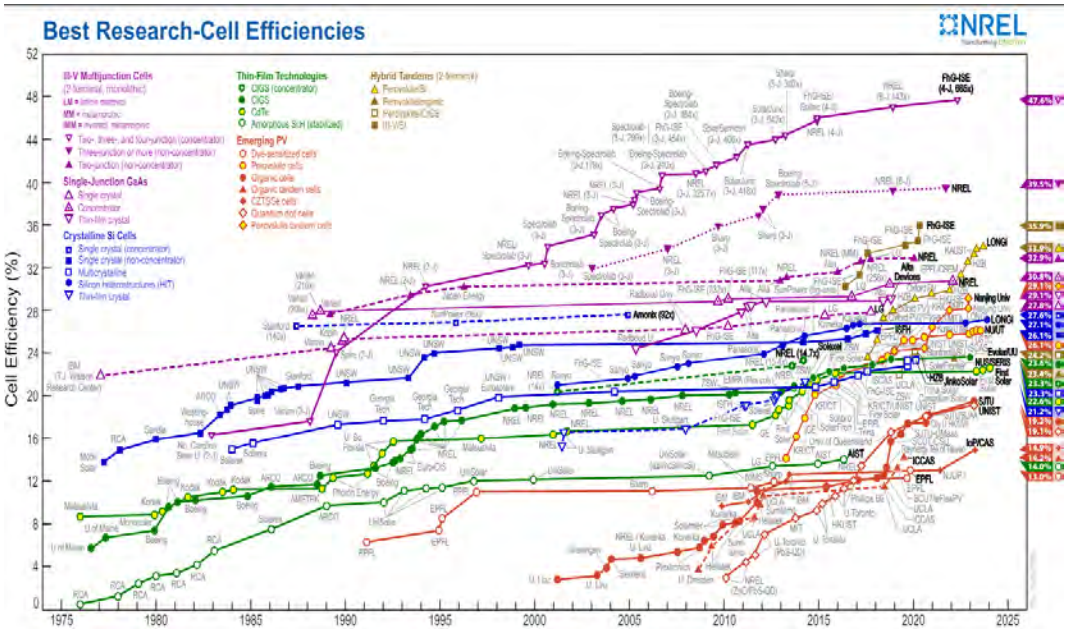

Figure 1. 3 NREL Efficiency Chart for Photovoltaic Technologies

Halide perovskites comprise a versatile family of materials represented by the chemical formula AMX_3. Where X denotes halogen anions, encompassing elements such as fluorine (F^-), chlorine (Cl^-), bromine (Br^-), and iodine (I^-), as shown in Fig 1.4. A denotes cations and can be occupied by monovalent alkali metals (Li^+, Na^+, K^+, Rb^+, Cs^+) or organic cations (like those found in amines or ammonium compounds). M corresponds to the divalent metal cation with common choices, including lead (Pb^{2+}), tin (Sn^{2+}), iron (Fe^{2+}), Germanium (Ge^{2+}), etc. The selection of metal strongly influences the perovskite's electronic and optical properties. The potential of perovskites for solar energy applications was first recognized by Salau in 1980. His research on $KPbI_3$ revealed a direct bandgap between 1.4 and 2.2 eV [44], a range well-suited for absorbing sunlight. Notably, the stability of a given perovskite structure is strongly influenced by the "tolerance factor." This formula, $t = (R_A + R_B)/ \{\sqrt{2}(R_B + R_X)\}$, takes into account the sizes of the A and B cations and the X anion [45].

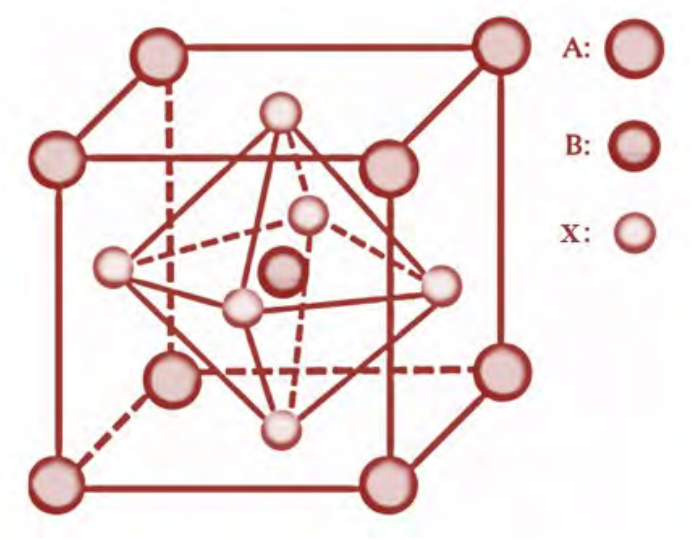

Figure 1. 4 Three-dimensional cubic perovskite of general formula AMX_3.

The tolerance factor serves as a valuable predictive tool for perovskite formation. In reality, the majority of perovskites possess minute structural imperfections. Even subtle deviations from the ideal tolerance factor due to the introduction of mild defects can profoundly impact the material's performance, affecting its electrical conductivity and magnetic response, among other properties. Understanding these flaws is crucial to create perovskites with the optimal characteristics suited for diverse applications.

In 1839, Gustav Rose discovered perovskite, a mineral found in Russia named after the mineralogist Aleksvich Von Perovski. In 2009, the initial use of perovskite as a material to absorb sunlight in solar cells led to extensive research into perovskite solar cells (PSCs) and resulted in significant advancements in efficiency. The exceptional efficacy of perovskite materials in absorbing sunlight, combined with their potential for cost-effective manufacturing, has sparked the interest of scientists and researchers. Lead-halide perovskites, in particular, displayed tremendous growth in efficiency and outpacing many established photovoltaic technologies. Despite impressive efficiencies, lead-based perovskites face challenges. Their organic components degrade under real-world conditions, hindering long-term use. Even more concerning is lead toxicity, posing environmental and health risks. Strict regulations, increasing awareness of environmental and health hazards, and a sense of responsibility within the scientific community drive the urgent need for alternatives [46,47]. The focus of research has shifted towards developing lead-free perovskite alternatives. This is vital for sustaining

the exceptional efficiency and cost-effective processing of perovskites, all while ensuring a clean and environmentally responsible future for solar energy [48-51]. The continued refinement and optimization of the lead-free options have the potential to unlock a new generation of eco-friendly solar cells without compromising performance. The remarkable story of perovskites demonstrates the relentless pursuit of innovation within the field of renewable energy. Their unique properties, adaptability, and vast potential will ensure that they remain at the forefront of scientific research. Overcoming the challenge of finding lead-free alternatives is the key to unlock a future where solar energy becomes not only prevalent but also sustainable, revolutionizing the way we power our world.

In response to these challenges, scientists are actively exploring safer and more stable alternatives that maintain the beneficial properties of lead perovskites. Several potential avenues have surfaced. Tin, which shares characteristics similar to lead, emerges as an obvious first choice. Researchers studied several tin-based perovskites such as $CsSnBr_3$, Cs_2SnI_6, and tin alloyed with germanium ($CsSn_xGe_{1-x}I_3$), etc., which shows exciting photo absorption capabilities comparable to their lead counterparts [52]. Despite its potential, tin-based perovskites frequently exhibit oxidation and instability issues, necessitating the introduction of dopants and additives to improve performance. Bismuth, alone or in double perovskite (elpasolite) formations, represents another potential option. These materials usually display higher stability, but their band gaps may be less suitable for solar applications. Copper-based perovskites and other unconventional formulations are also being investigated. Each technique has distinct compromises in efficiency, stability, and ease of manufacture. The ongoing quest for lead-free perovskites underscores a commitment to sustainability and their long-term viability. Although no single option has fully matched the performance of lead-based perovskites, research into novel techniques and materials is generating encouraging results. This study exemplifies the persistent drive in the renewable energy field to develop solutions that are efficient, safe, and responsible.

1.3.2 Organic-inorganic Sn-based halide perovskites

Methylammonium lead iodide ($MAPbI_3$) has been at the forefront of perovskite solar cell research since its potential was first recognized. These crystal structures combine the organic cation methylammonium ($CH_3NH_3^+$), divalent lead (Pb^{2+}), and three iodide

anions (I^-) [53]. $MAPbI_3$ perovskites exhibit excellent optical and electronic properties, with a band gap of 1.55-1.64 eV, carrier diffusion lengths exceeding 100 nm, and low exciton binding energies of 10-24 meV [54]. The first use of $MAPbI_3$ in solar cells was reported by Kojima et al. in 2009 [38], marking the beginning of a new era in photovoltaics. In 2012, Lee et al. demonstrated the first completely solid-state perovskite solar cell, further showcasing the material's potential [55]. By employing effective doping, passivation, and encapsulation techniques, devices using $MAPbI_3$ have achieved power conversion efficiencies (PCEs) exceeding 25%. However, $MAPbI_3$ has some drawbacks. It is thermally unstable and degrades in humid environments, and the lead content raises environmental and health concerns.

Metals belonging to groups 14-15, like tin (Sn), germanium (Ge), antimony (Sb), and bismuth (Bi) have the potential to substitute lead in PSCs due to similar semiconducting properties [56-59]. Among these options, Sn (II)-based halide perovskites have demonstrated the highest power conversion efficiency and generated significant interest in the perovskite solar cell industry. Sn-based perovskite solar cells, such as methylammonium tin iodide ($MASnI_3$), formamidinium tin iodide ($FASnI_3$), and cesium tin iodide ($CsSnI_3$), have a marginal and more appealing direct bandgap than lead-based perovskite solar cells [60]. In case of Pb-based Perovskite, Pb^{2+} degrades to Pb^{4+} and oxidizes to PbO_2, which is a harmful toxic gas and lethal to the environment. On the other hand, in Sn-based PSCs, Sn^{2+} degrades to Sn^{4+} and oxidizes to SnO_2, making it ecofriendly and a viable alternative for lead. These two types of perovskites (Tin/Lead-based) share similar significant physical properties [61-63]. The similar size of Sn^{2+} (1.35 Å) compared to Pb^{2+} (1.49 Å) allows seamless substitution of lead with tin within the perovskite crystal structure. This change results in smaller bandgaps, a desirable attribute for solar cells as it broadens the range of light that can be absorbed for higher theoretical efficiency.

Despite having a similar structure and comparable bandgap to $MAPbI_3$, $MASnI_3$ perovskite solar cells have struggled with low efficiency and poor stability. Tin tends to exist in multiple oxidation states, leading to defects and non-radiative recombination centers that degrade performance. Early efforts to stabilize $MASnI_3$ involved using antioxidant additives, surface passivation techniques, and careful control of the fabrication environment to minimize oxygen and moisture. Despite these challenges,

the efficiency of $MASnI_3$-based perovskite solar cells has significantly improved in recent years. Researchers have developed new synthetic routes, explored various dopants, and employed innovative device architectures to enhance the PCE and longevity of $MASnI_3$ solar cells. In 2014, Snaith et al. reported the first $MASnI_3$-based solar cells with a maximum efficiency of 6.4% and an average efficiency of less than 2% [64]. Zhao et al. later fabricated $MASnI_3$ and $FASnI_3$ devices in a normal n-i-p structure, achieving efficiencies of 0.16% and 0.65%, respectively [65-66]. However, recent years have seen an accelerated improvement in $MASnI_3$ solar cell efficiency. Fabrication techniques like the modified solvent bathing method have been used to improve the coverage and stability of $MASnI_3$ films, achieving PCEs of 2.14% with long lifetimes over 200 hours under 1 Sun conditions (AM1.5, 100 mW/cm^2) [67]. Hollow $MASnI_3$ perovskite-based solar cells have also been investigated, achieving high reproducible efficiencies of up to 6.63% and open-circuit voltages of 428.67 mV [68]. The use of two-dimensional materials like graphene in $MASnI_3$ devices has further enhanced performance and stability. Jen et al. demonstrated the fabrication of Sn-based perovskite solar cells in both normal and inverted structures [69]. They enhanced the performance by incorporating trimethyl iodide into $FASnI_3$, achieving a notable efficiency of 7.09% in the inverted structure. In contrast, the normal structure yielded only 4.43% efficiency despite the implementation of a thin C_{60}-coated SnO_2 electron-selective layer. This modification effectively facilitated electron transport, contributing to the functionality of Sn-based PSCs. Additionally, Xu et al. developed $FASnI_3$-based solar cells using a normal n-i-p structure [70]. The highest reported experimental efficiency for $MASnI_3$-based perovskite solar cells is 14.6% [71]. In addition, using numerical simulation, Kumar et al. reported optimized $MASnI_3$ devices with a theoretical PCE of 27% [72]. Achieving these high efficiencies required relatively complex fabrication techniques, including the addition of various buffer layers and sophisticated band alignment strategies, which may increase the overall cost of producing these PSCs.

1.3.3 Inorganic Sn-based halide perovskites

While organic-inorganic hybrid PSCs, particularly those based on $MASnI_3$, have achieved remarkable progress, their inherent limitations remain a hurdle for commercialization. Organic components within these structures exhibit volatility,

leading to rapid degradation of the perovskite upon exposure to moisture. Consequently, relying solely on organic-inorganic lead-free architectures, similar to $MAPbI_3$, may not be a viable long-term solution. To overcome this challenge, researchers are concentrating on the development of fully inorganic perovskite solar cell materials. Notably, Cs-based inorganic perovskites, such as $CsSnX_3$ (where X represents a halogen), have emerged as promising candidates for lead-free, inorganic PSCs, demonstrating excellent potential to maintain high efficiencies without compromising environmental safety. Sabba et al. observed an evolution in crystal structure and bandgap, progressing from $CsSnI_3$ (1.27 eV) to $CsSnI_2Br$ (1.37 eV), $CsSnIBr_2$ (1.65 eV), and $CsSnBr_3$ (1.75 eV). Among these, $CsSnI_3$ shows promise for PSCs due to its narrow bandgap and excellent optoelectronic properties, with predicted theoretical PCEs of up to 23%. Tin-based perovskite solar cells often exhibit short-circuit current densities (J_{SC}) in the range of 20 to 25 mA/cm^2. However, their open-circuit voltage (V_{OC}) is approximately 0.5 V, owing to their narrow bandgaps, significantly lower than the 1.1 V observed in lead-based perovskites. Researchers are actively addressing these challenges to enhance the stability and photovoltaic output of inorganic tin-based PSCs [73–75].

1.3.4 Inorganic Ge-based halide perovskites

Ge has an electrical structure comparable to Pb and Sn; however, the ion radius of Ge^{2+} is significantly smaller (0.73 Å). Inorganic Ge-based perovskites have better ionic conductivity and wider bandgaps than the equivalent Pb or Sn-based perovskites. The bandgaps of $CsGeCl_3$, $CsGeBr_3$, and $CsGeI_3$ were calculated to be 3.67, 2.32, and 1.53 eV, respectively, indicating that $CsGeI_3$ might be used as a photovoltaic absorber. Liu et al. found that $CsGeI_3$'s bandgap can vary between 0.73 and 2.3 eV depending on the strain [76]. Quan et al. observed that the Pmmm structure of $CsGeI_3$ gradually changed to R3m when the temperature decreased due to the position deviation of Ge and I atoms [77]. They explored the phase transformation of newly synthesized $CsGeI_3$ nanocrystals under an electron beam, noting a progression from single-crystalline $CsGeI_3$ to single-crystalline CsI and eventually to polycrystalline CsI fragments [77]. Kopacic et al. demonstrated that partial I substitution with Br could limit the deterioration of Ge-based perovskites [78]. However, there are still few studies on $CsGeI_3$-based PSCs. Raj et al. evaluated the performance of $CsGeI_3$ PSCs using SCAPS simulation and found that the

maximum feasible PCE was 18.3% with J_{SC} of 23.31 mA/cm^2, V_{OC} of 1.04 V, and FF of 75.46% [79]. They next simulated the photovoltaic performance of $CsGeI_3$ PSCs with various electron transport layers (ETLs), and the devices with C_{60} and SnO_2 ETLs achieved PCEs of 8.45% and 8.46%, respectively [80]. Krishnamoorthy et al. announced the first $CsGeI_3$-based PSC in 2015, with just 0.11% PCE achieved due to Ge^{2+} oxidation during manufacturing methods [81]. Later, Chen et al. synthesized high-quality $CsGeX_3$ (X = Cl, Br, I) quantum rods using a solvothermal process, providing high-efficiency Ge-based PSCs with PCEs of 4.94%, 4.92%, and 2.57% for $CsGeI_3$, $CsGeBr_3$, and $CsGeCl_3$, respectively [82]. Future directions for manufacturing high-performance Ge-based PSCs include investigating efficient methods for obtaining high-quality $CsGeI_3$ or Ge-based alloying perovskite films and stabilizing their lattice.

1.4 Different components of a Perovskite solar cell

1.4.1 Transparent Conducting Oxide (TCO)

The TCO layer in a perovskite solar cell plays a two-fold role. First, it acts as a transparent window, allowing sunlight to reach the light-harvesting perovskite layer. Second, it functions as a critical current collector, efficiently gathering and channeling the generated electrons for further processing within the device. Electrons originating from the perovskite layer reach the TCO substrate through the electron transport layer [83]. The TCO must possess excellent optical transparency to transmit light to the photoactive perovskite layer. Indium Tin Oxide (ITO) and Fluorine-doped Tin Oxide (FTO) are commonly used key materials as TCO layers in perovskite solar cells.

1.4.2 Electron Transport Layer (ETL)

In perovskite solar cells, the efficient transport of charges is influenced significantly by the energy level alignment between the work function of the transporting electrode and the active layer. Ultrathin charge transport materials are introduced between the active layer and the electrodes to achieve proper energy level alignment [84]. N-type semiconductor metal oxides like TiO_2, ZnO, SnO_2, WO_3, and ZrO_2 are commonly used as electron transport materials due to their low work functions and excellent chemical stability against perovskite precursor solutions. Incorporating a metal oxide layer within perovskite solar cells demonstrates a strategic adaptation from earlier dye-

sensitized solar cell (DSSC) designs. The electron transport layer serves a dual function in perovskite solar cells. First, it selectively extracts electrons from the perovskite layer and acts as a hole-blocking layer at the surface of the negative electrode. Second, it provides a larger surface area to accommodate perovskite crystals, enhancing the efficiency of charge transport and collection within the device [85]. Incorporating porous materials like Al_2O_3, ZrO_2, MoO_3, etc., between the perovskite layer and electron transport layer has been shown to improve the open-circuit voltage (V_{OC}) and overall device performance by facilitating better charge carrier extraction and reducing recombination losses [86].

1.4.3 Hole Transport Layer (HTL)

The Hole Transport Layer (HTL) in perovskite solar cells is crucial in transferring photogenerated holes from the perovskite layer to the counter electrode. Within perovskite solar cells, the HTM layer serves several essential purposes:

1. It acts as a physical and energetic barrier, preventing unwanted electron transfer and improving device stability.

2. With high hole mobility (often exceeding 10^{-3} $cm^2V^{-1}s^{-1}$) and carefully aligned energy levels, the HTM facilitates efficient hole transport to the electrode, improving overall efficiency [87].

3. The HTM protects the sensitive perovskite layer from degradation and corrosion that could occur at the metal contact.

4. Separating the perovskite from the top contact, the HTM helps minimize charge recombination, enhancing cell performance [88].

HTMs are available in diverse forms, comprising both organic-based and inorganic-based materials. Organic-based HTMs are categorized into long-chain polymers and small molecules, while inorganic HTMs include nickel, copper, p-type semiconductor, transition metal, and carbonaceous-based materials. Each category presents distinct advantages and properties tailored to enable efficient hole transport in perovskite solar cells.

1.4.4 Counter Electrode

The counter electrode used in perovskite solar cells must meet specific criteria: (i) it should remain inert when in contact with the hole transporting material, (ii) demonstrate high conductivity, and (iii) establish a Schottky barrier [89]. Its primary role is to gather and transfer charge from the external circuit back to the transporting layer, providing superior conductivity. Additionally, the counter electrode's work function significantly influences the desired built-in voltage of the solar cell device [90]. Various materials serve as counter electrodes in perovskite solar cell fabrication, including gold (Au), silver (Ag), aluminum (Al), platinum-doped FTO, and carbon-based materials. Each material choice offers specific advantages and may be selected based on factors such as cost-effectiveness, availability, and performance requirements. Due to its exceptional catalytic activity, platinum-coated FTO is conventionally used as the counter electrode in perovskite solar cells. However, the high cost and limited availability of platinum (Pt) have prompted recent efforts to identify low-cost, readily available substitutes for this critical component. Materials such as graphite, carbon black, activated carbon on FTO-glass, and organic-ion-doped conducting polymers like poly (3,4-ethylene dioxythiophene) (PEDOT) on both ITO and FTO-glass have emerged as viable options for counter electrode materials in Solar Cells [91-95]. However, challenges remain regarding adhesion to the substrate surface and opacity associated with carbon-based counter electrodes. Continued research focuses on overcoming these challenges and optimizing counter-electrode materials to enhance the performance of PSCs.

1.4.5 Device Architecture of Perovskite Solar Cells

A standard perovskite solar cell device comprises several key components. At its core is the photoactive absorber layer, commonly called the perovskite layer, typically with a thickness of a few hundred nanometers. This layer is sandwiched between two selective transporting layers: one that facilitates the flow of electrons (electron transport layer) and another that blocks electrons while allowing the passage of holes (hole transport layer). These layers work together to facilitate the efficient movement of charge carriers within the device. The device structure is completed with two

conductive electrodes positioned at each end. One electrode is optically transparent, allowing incoming light to penetrate and reach the perovskite layer. The other electrode acts as the collection point for the generated electrical charge. This design ensures that the current produced by the solar cell can be effectively harnessed.

1.5 Working Principle of Solar Cells

Solar cells operate on the fundamental principle of converting solar energy into electrical energy. The initial step in perovskite solar cell operation involves light absorption by the active perovskite layer. Incident photons, characterized by their energy quanta *hv* (where h is Planck's constant and *v* is the frequency), interact with the electronic structure of the perovskite material. This process creates an electron-hole pair, termed an exciton, where the "hole" represents the vacancy left behind in the valence band. These Coulombically bound excitons serve as the primary charge carriers within the device and are key for initiating the subsequent steps of photocurrent generation. The operation of a solar cell can be described in three main steps: generation, separation, and transfer of charge carriers. The generation of charge carriers occurs when the semiconductor material absorbs incident photons. Subsequently, the charge carriers are separated, with electrons moving toward the electron transport layer (ETL) and holes toward the hole transport layer (HTL). In conclusion, the charge carriers undergo transfer within the device, which is facilitated by the presence of both the working and counter electrodes.

1.5.1 Absorption of Incident Photons

When light interacts with a semiconductor material, a portion is reflected, and some is transmitted through it. However, our main interest lies in the portion of light absorbed by the sensitizing material. This absorbed light energy is decisive for generating charge carriers within the semiconductor material, which is crucial for the operation of the solar cell [96].

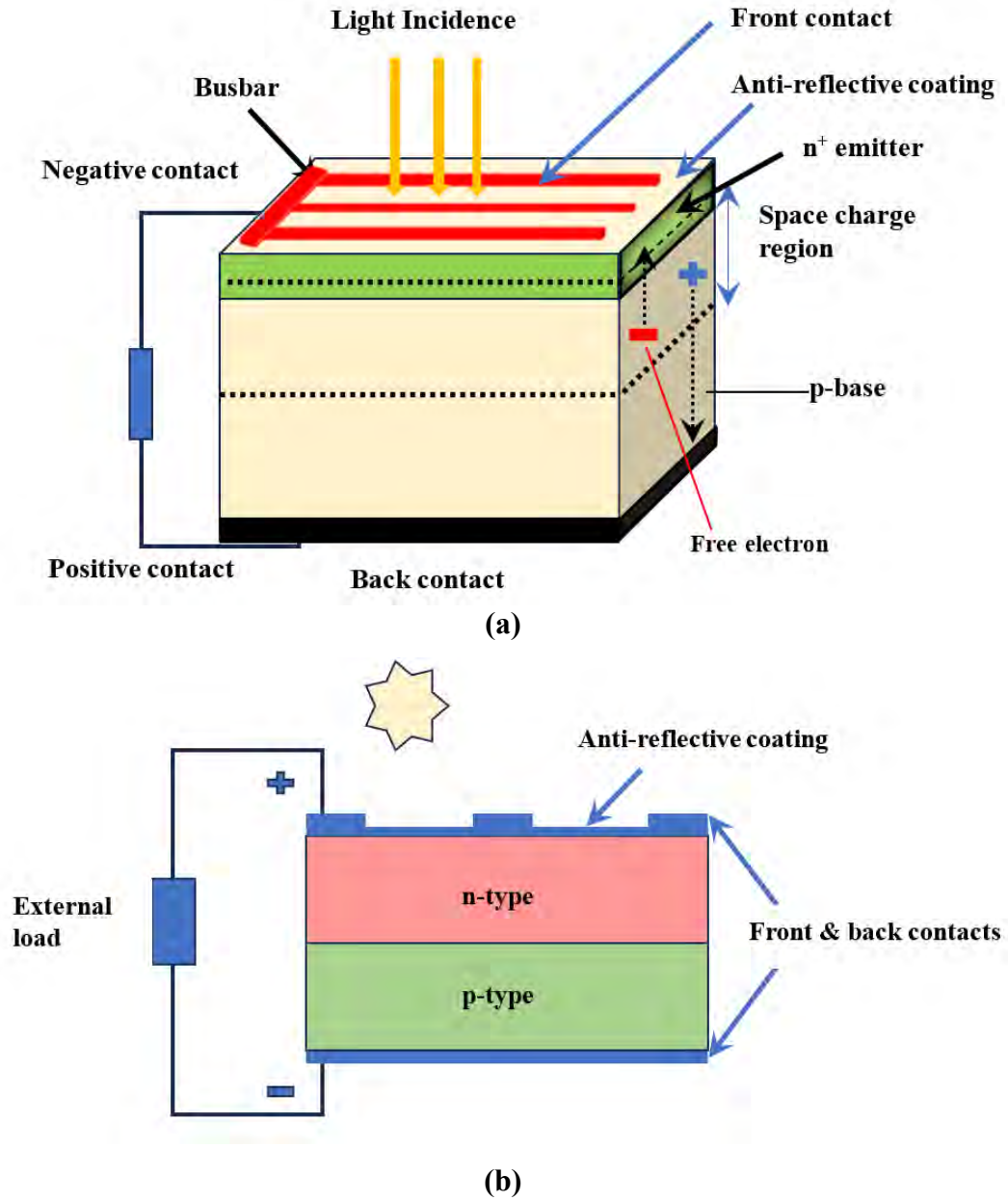

Figure 1. 5(a) Schematic of Conventional Solar Cell (b) Two-dimensional (2D) cross-section of a conventional solar cell. Taken from

The diagram depicts the structure of the solar cell (Fig. 1.**5**). When sunlight reaches the photovoltaic cell, it arrives as electromagnetic radiation, comprised of individual units of light called photons. Each photon carries energy, represented as $h\nu$ and defined in equation 1.1. As per de Broglie's hypothesis, photons demonstrate both particle-like and wave-like attributes, with a specific wavelength denoted as λ. Consequently, the energy $E(\lambda)$ of a photon is defined by the equation:

$$E(\lambda) = h\nu = hc/\lambda \qquad (1.1)$$

Here, h represents Planck's constant, and c represents the speed of light. Not all incident photons make a direct contribution to the generation of electrical energy. Only photons with energies surpassing the band gap of the semiconductor material can generate electron-hole pairs, thereby transforming light energy into electrical energy. Consequently, the spectral composition of electromagnetic radiation plays an essential role in determining the efficiency of solar cells.

1.5.2 Generation of Free Electrons and Holes

The generation of electron-hole pairs (EHP) in solar cells is an important process that explains how they operate. When a light source with high energy illuminates a crystal, it causes changes in its electrical properties. This intense light disrupts the stable positions of bound electrons within the crystal, setting them free to move. When electrons separate from their bonds, they create empty spaces called holes. These free electrons move through the crystal's conduction band, creating an electric current as they pass through a circuit. Both the conduction-band electrons and the holes are essential for the solar cell's efficient operation, significantly influencing its electrical behavior. Together, they form what is known as the light-generated electron-hole pair, which can freely traverse the crystal. The movement of holes in a material is indirectly influenced by the behavior of neighboring electrons. As free electrons move in one direction, electrons from adjacent areas fill the holes, effectively causing the holes to move in the opposite direction. When a free electron creates a hole, an electron from a nearby bond can fill the vacancy left by the free electron (hole), creating a new vacancy or hole. This process continues, with each electron filling a vacancy, appearing as if the hole has shifted its position. This phenomenon persists, particularly as the material's temperature rises, leading to increased thermal agitation of electrons and holes and, consequently, more movement. While the photogeneration of electron-hole pairs is a fundamental prerequisite for solar cell operation, it alone does not guarantee efficient energy conversion. Without a charge separation mechanism, photogenerated EHPs will likely undergo recombination processes, dissipating their acquired energy as heat. Therefore, a built-in potential barrier is indispensable for effective charge separation, inhibiting recombination and facilitating the extraction of electrons and holes at their respective electrodes, thus enabling the generation of photocurrent.

1.5.3 Transport of Photo Generated Carriers

As discussed earlier, in addition to generating EHPs, a built-in potential barrier is essential for the effective operation of a solar cell. This barrier plays a critical role in

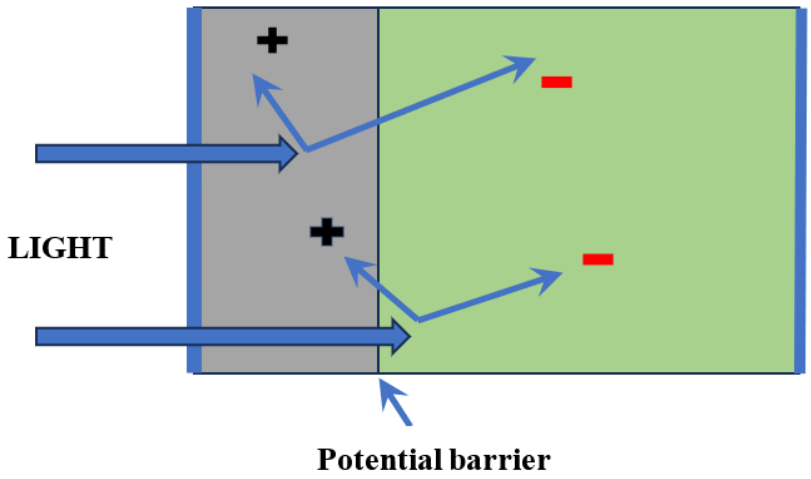

Figure 1. 6 Separation of Light-Generated Charge Carriers

separating charges, thereby reducing the chances of electron-hole recombination. This potential barrier is established in a photovoltaic cell due to the presence of opposite types of charges on either side, namely the p-type and n-type regions. The space charge region formed by this arrangement selectively directs more electrons toward the n-side and more holes toward the p-side of the cell, as shown in Fig 1.6. By separating these charges, the potential barrier minimizes the chances of recombination, allowing the charges to retain their energy. Instead, as the charges separate, a potential difference is established across the cell, creating an electric field that drives the flow of electric current. This current flow is the fundamental mechanism by which solar cells convert light energy into electrical energy [97].

1.5.4 Collection of Photogenerated Carriers

A space charge region forms at the junction of the p-type and n-type semiconductors in a solar cell, creating an inherent potential known as the junction barrier. When a free electron enters this region, it is driven toward the n-type region due to the electric field. In the n-type region, where holes are minority carriers, the probability of recombination is significantly diminished. Additionally, the electron faces resistance to return to the p-type region due to the repulsive forces generated by the junction field. The built-in

potential barrier actively guides the hole towards the p-type region, preventing it from recombining with an electron in the n-type region. This separation is crucial for preserving the generated charge carriers and maximizing electrical output. When light strikes the n-side of the junction, the newly formed electron-hole pairs increase the electron count as the holes migrate to the p-side, where they can move freely. Therefore, the initial step in a semiconductor exposed to light involves charge formation, followed by charge separation facilitated by the junction barrier. This charge separation is critical. Without it, excited electrons and holes would immediately recombine, negating the energy gained from sunlight. The separation process effectively creates an imbalance of charges within the cell. Electrons accumulate on the n-type side, while holes gather on the p-type side. This imbalance creates a voltage difference (electromotive force) across the junction. This voltage difference is what drives the flow of electricity when the solar cell is connected to a circuit. Electrons flow from the n-type region (negative) to the p-type region (positive) through an external wire, generating an electric current.

Marchioro et al. [98] proposed that electron-hole pairs generated at the interfaces of the electron transport layer (ETL)/perovskite and hole transport layer (HTL)/perovskite undergo separation, with electrons injected into the ETL (process (i) in Fig. 1.7) and holes injected into the HTL (process (ii)) to facilitate charge transport [99]. However, several detrimental behaviors to the cell's performance may also occur, including exciton annihilation (process (iii)), photoluminescence, nonradiative recombination, reverse transmission of electrons and holes (process (iv) and (v)), and recombination at the ETL/HTL interface (process (vi)). The transport processes of electrons and holes in an HTL/perovskite/ETL cell are illustrated in Fig. 1.7.

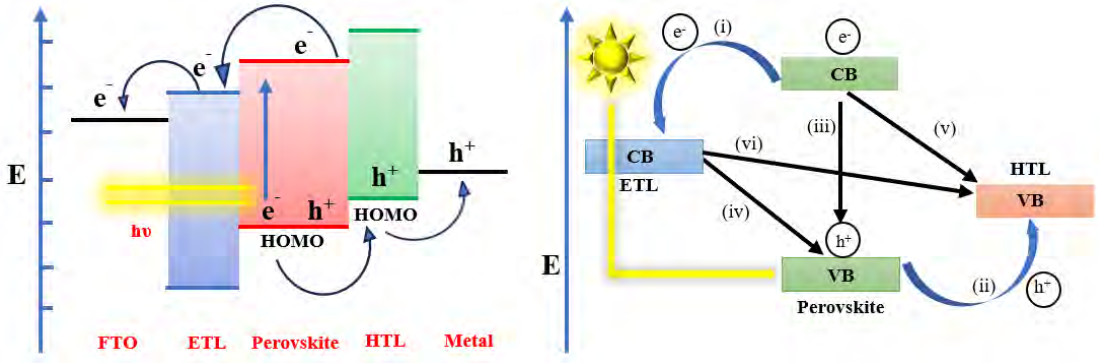

Figure 1. 7 Schematic diagram of energy levels and transport processes of electrons and holes in an HTM/Perovskite/ETL cell.

1.6 Scope of the Thesis

This thesis embarks on a journey to redefine the landscape of solar energy technology by focusing on the transition from lead-based to lead-free perovskite solar cells (PSCs). The global demand for sustainable and clean energy solutions has never been more critical, and this research addresses the environmental and economic challenges posed by traditional silicon-based photovoltaics. By exploring novel lead-free organic-inorganic hybrid materials and innovative fabrication techniques, this study aims to enhance the stability, efficiency, and sustainability of PSCs. Additionally, the theoretical exploration of fully inorganic perovskite-based solar cells aims to establish a solid foundation for future advancements in this promising field. Employing an extensive array of experimental techniques and theoretical tools, including Density Functional Theory (DFT) and SCAPS-1D simulations, this research precisely characterizes and optimizes the materials used in PSCs. The focus on novel materials such as $MASnI_3$, $CsGeI_XBr_{3-X}$, and $RbSnI_3$, combined with innovative strategies like metal doping and the formation of $CsSnI_3/CsSnBr_3$ heterostructures, aims to significantly enhance photovoltaic performance. The primary focus is to establish a foundation for future progress by integrating the theoretical estimations with the experimental observations. In conclusion, this work aspires to contribute to the development of eco-friendly, cost-effective, and highly efficient solar energy solutions. By addressing critical issues such as lead toxicity, material stability, and device efficiency, the insights gained from this study are expected to pave the way for future innovations, ultimately fostering the widespread adoption of sustainable energy technologies.

References

(1) Patel, Nikul K., and Shailesh N. Shah. "Biodiesel from plant oils." In Food, energy, and water, pp. 277-307. Elsevier, 2015.

(2) European Commission, The Energy Challenge of the 21st Century: The role of Nuclear Energy, http://europa.eu.int/comm/research/rtdinfo en.html

(3) M. Grätzel, Solar Energy Conversion by Dye-Sensitized Photovoltaic Cells, Inorg. Chem., 2005, 44(20), 6841–6851

(4) Dobber, M., Voors, R., Dirksen, R., Kleipool, Q., & Levelt, P. (2008). The high-resolution solar reference spectrum between 250 and 550 nm and its application to measurements with the Ozone Monitoring Instrument. Solar Physics, 249, 281-291.

(5) Meftah, M., Damé, L., Bolsée, D., Pereira, N., Snow, M., Weber, M., ... & Bekki, S. (2020). A new version of the SOLAR-ISS spectrum covering the 165–3000 nm spectral region. Solar Physics, 295, 1-16.

(6) Song, Dengyuan, Jingfeng Xiong, Zhiyan Hu, Gaofei Li, Hongfang Wang, Haijiao An, Bo Yu et al. "Progress in n-type Si solar cell and module technology for high efficiency and low cost." In 2012 38th IEEE Photovoltaic Specialists Conference, pp. 003004-003008. IEEE, 2012.

(7) T. Saga, "Advances in crystalline silicon solar cell technology for industrial mass production," NPG Asia Mater. 2 (2010) 96–102

(8) K. L. Chopra, P. D. Paulson, and V. Dutta, "Thin-film solar cells: an overview," Prog. Photovolt. Res. Appl. 12 (2004) 69–92

(9) M. A. Green, "Third generation photovoltaics: advanced solar energy conversion. Berlin" Springer (2006)

(10) Conibeer, G 2007, 'Third-generation photovoltaics', Materials today, vol. 10, no. 11, pp. 42-50.

(11) Lin, H., Yang, M., Ru, X., Wang, G., Yin, S., Peng, F., ... & Xu, X. (2023). Silicon heterojunction solar cells with up to 26.81% efficiency achieved by electrically optimized nanocrystalline-silicon hole contact layers. Nature Energy, 8(8), 789-799.

(12) Avrutin, V., N. Izyumskaya, and H. Morkoç. "Semiconductor solar cells: Recent progress in terrestrial applications." Superlattices and Microstructures 49, no. 4 (2011): 337-364.

(13) Aberle, Armin G. “Thin-film solar cells.” Thin solid films 517, no. 17 (2009): 4706-4710.

(14) Pagliaro, Mario, Giovanni Palmisano, and Rosaria Ciriminna. Il nuovo fotovoltaico. Palermo: Dario Flaccovio Editore, 2008.

(15) Gloeckler, M., I. Sankin, and Z. Zhao. “CdTe solar cells at the threshold to 20% efficiency.” IEEE Journal of Photovoltaics 3, no. 4 (2013): 1389-1393.

(16) Pagliaro, Mario, Giovanni Palmisano, and Rosaria Ciriminna. Il nuovo fotovoltaico. Palermo: Dario Flaccovio Editore, 2008.

(17) https://www.pv-magazine.com/2021/03/04/avancis-claims-19-64- efficiency-for-cigs-module/

(18) Green, Martin, Ewan Dunlop, Jochen Hohl-Ebinger, Masahiro Yoshita, Nikos Kopidakis, and Xiaojing Hao. “Solar cell efficiency tables (version 57).” Progress in photovoltaics: research and applications 29, no. 1 (2021): 3-15.

(19) Nakamura, Motoshi, Koji Yamaguchi, Yoshinori Kimoto, Yusuke Yasaki, Takuya Kato, and Hiroki Sugimoto. “Cd-free Cu (In, Ga)(Se, S) 2 thin-film solar cell with record efficiency of 23.35%.” IEEE Journal of Photovoltaics 9, no. 6 (2019): 1863-1867.

(20) Jackson, Philip, Roland Wuerz, Dimitrios Hariskos, Erwin Lotter, Wolfram Witte, and Michael Powalla. “Effects of heavy alkali elements in Cu (In, Ga) Se2 solar cells with efficiencies up to 22.6%.” physica status solidi (RRL)–Rapid Research Letters 10, no. 8 (2016): 583-586.

(21) Plentz, Jonathan, Gudrun Andrä, Torsten Pliewischkies, Uwe Brückner, Björn Eisenhawer, and Fritz Falk. "Amorphous silicon thin- film solar cells on glass fiber textiles." Materials Science and Engineering: B 204 (2016): 34-37.

(22) Zhang, Yaokang, Sze-Wing Ng, Xi Lu, and Zijian Zheng. “Solution- processed transparent electrodes for emerging thin-film solar cells.” Chemical Reviews 120, no. 4 (2020): 2049-2122.

(23) Arumugam, Sasikumar, Yi Li, Monika Glanc-Gostkiewicz, Russel N. Torah, and Stephen P. Beeby. “Solution processed organic solar cells on textiles.” IEEE Journal of Photovoltaics 8, no. 6 (2018): 1710-1715.

(24) GREENY, Martin A., Keith Emery, Yoshihiro Hishikawa, and Wilhelm Warta. “Solar cell efficiency tables (version 37).” Progress in photovoltaics 19, no. 1 (2011): 84-92.

(25) Itzhaik, Yafit, Olivia Niitsoo, Miles Page, and Gary Hodes. “Sb2S3- sensitized nanoporous TiO2 solar cells.” The Journal of Physical Chemistry C 113, no. 11 (2009): 4254-4256.

(26) Lévy-Clément, Claude. “Nanostructured ETA-solar cells.” In Nanostructured Materials for Solar Energy Conversion, pp. 447-484. Elsevier, 2006.

(27) Lévy-Clément, Claude, Ramon Tena-Zaera, Margaret A. Ryan, Abou Katty, and Gary Hodes. “CdSe-sensitized p-CuSCN/nanowire n-ZnO heterojunctions.” Advanced Materials 17, no. 12 (2005): 1512-1515.

(28) Chandrasekaran, J., D. Nithyaprakash, K. B. Ajjan, S. Maruthamuthu, D. Manoharan, and S. Kumar. “Hybrid solar cell based on blending of organic and inorganic materials—An overview.” Renewable and Sustainable Energy Reviews 15, no. 2 (2011): 1228-1238.

(29) Chandrasekaran, J., D. Nithyaprakash, K. B. Ajjan, S. Maruthamuthu, D. Manoharan, and S. Kumar. “Hybrid solar cell based on blending of organic and inorganic materials—An overview.” Renewable and Sustainable Energy Reviews 15, no. 2 (2011): 1228-1238.

(30) Gong, Jiawei, Jing Liang, and K. Sumathy. “Review on dye-sensitized solar cells (DSSCs): fundamental concepts and novel materials.” Renewable and Sustainable Energy Reviews 16, no. 8 (2012): 5848- 5860.

(31) Upadhyaya, Hari M., S. Senthilarasu, Min-Hung Hsu, and D. Kishore Kumar. “Recent progress and the status of dye-sensitised solar cell (DSSC) technology with state-of-the-art conversion efficiencies.” Solar Energy Materials and Solar Cells 119 (2013): 291-295.

(32) Li, Bin, Liduo Wang, Bonan Kang, Peng Wang, and Yong Qiu. “Review of recent progress in solid-state dye-sensitized solar cells.” Solar energy materials and solar cells 90, no. 5 (2006): 549-573.

(33) Li, Qinghua, Haiyan Chen, Lin Lin, Pinjiang Li, Yuancheng Qin, Mingjun Li, Benlin He, Lei Chu, and Qunwei Tang. “Quasi-solid-state dye-sensitized solar cell from polyaniline integrated poly (hexamethylene diisocyanate tripolymer/polyethylene glycol) gel electrolyte.” Journal of Materials Chemistry A 1, no. 17 (2013): 5326- 5332.

(34) Kawano, Ryuji, Hiroshi Matsui, Chizuru Matsuyama, Akihiro Sato, Md Abu Bin Hasan Susan, Nobuo Tanabe, and Masayoshi Watanabe. “High performance

dye-sensitized solar cells using ionic liquids as their electrolytes." Journal of Photochemistry and Photobiology A: Chemistry 164, no. 1-3 (2004): 87-92.

(35) Angaiah, Subramania, Vignesh Murugadoss, Subasri Arunachalam, Pratheep Panneerselvam, and Sarathkumar Krishnan. "Influence of various ionic liquids embedded electrospun polymer membrane electrolytes on the photovoltaic performance of DSSC." Engineered Science 4, no. 16 (2018): 44-51.

(36) Saito, Yasuteru, Norihiro Fukuri, Rohan Senadeera, Takayuki Kitamura, Yuji Wada, and Shozo Yanagida. "Solid state dye sensitized solar cells using in situ polymerized PEDOTs as hole conductor." Electrochemistry communications 6, no. 1 (2004): 71-74.

(37) Wang, Yanping, Ke Yang, Seong-Cheol Kim, Ramaswamy Nagarajan, Lynne A. Samuelson, and Jayant Kumar. "In situ polymerized carboxylated diacetylene as a hole conductor in solid-state dye- sensitized solar cells." Chemistry of materials 18, no. 18 (2006): 4215- 4217.

(38) Kojima A, Teshima K, Shirai Y, Miyasaka T (2009) Organometal halide perovskites as visible-light sensitizers for photovoltaic cells. J Am Chem Soc 131:6050–6051.

(39) Ono LK, Qi Y (2016) Surface and Interface Aspects of Organometal Halide Perovskite Materials and Solar Cells. Journal of Physical Chemistry Letters 7:4764–4794.

(40) Seo J, Noh JH, Seok S Il (2016) Rational Strategies for Efficient Perovskite Solar Cells. Acc Chem Res 49:562–572.

(41) Deng X, Xie L, Wang S, et al (2020) Ionic liquids engineering for high-efficiency and stable perovskite solar cells. Chemical Engineering Journal 398:125594.

(42) Huang Y, Liu T, Liang C, et al (2020) Towards Simplifying the Device Structure of High-Performance Perovskite Solar Cells. Adv Funct Mater 30:2000863.

(43) Green MA, Dunlop ED, Yoshita M, et al (2024) Solar cell efficiency tables (Version 63). Progress in Photovoltaics: Research and Applications 32:3–13.

(44) A. M. Salau, "Fundamental absorption edge in PbI2:KI alloys", Solar Energy Materials 2 (1980) 327-332

(45) Goldschmidt, Victor M., et al. "Geochemische verteilungsgesetze der elemente VII." Skrifter der Norske Videnskaps Akademi Klasse 1. Matematisk Naurvidenskaplig Klasse (1926).

(46) Schileo, G., & Grancini, G. (2021). Lead or no lead? Availability, toxicity, sustainability and environmental impact of lead-free perovskite solar cells. Journal of materials chemistry C, 9(1), 67-76.

(47) Li, G., Price, M., & Deschler, F. (2016). Research Update: Challenges for high-efficiency hybrid lead-halide perovskite LEDs and the path towards electrically pumped lasing. APL Materials, 4(9).

(48) Jiang, X., Li, H., Zhou, Q., et al., 2021. One-Step Synthesis of SnI2・(DMSO)x Adducts for High-Performance Tin Perovskite Solar Cells. J. Am. Chem. Soc. 143, 10970–10976.

(49) Li, M., Li, F., Gong, J., Zhang, T., Gao, F., Zhang, W.-H., Liu, M., 2022. M. Advances in Tin (II)-Based Perovskite Solar Cells: From Material Physics to Device Performance. Small Struct. 3 (1), 2100102.

(50) Yu, B., Chen, Z., Zhu, Y., et al., 2021. Heterogeneous 2D/3D Tin-Halides Perovskite Solar Cells with Certified Conversion Efficiency Breaking 14%. Adv. Mater. 33, 2102055.

(51) Cao, J., Yan, F., 2021. Recent progress in tin-based perovskite solar cells. Energy Environ. Sci. 14, 1286–1325.

(52) Nakamanya, B., Kakooza, T., Sun, Q., Haghayegh, M., BALILONDA, A., Tebyetekerwa, M., ... & Zhu, M. (2024). Strategies Towards High-Performance Tin-Based Perovskite Solar Cells. Journal of Materials Chemistry C.

(53) Jaffe, A., Lin, Y., Beavers, C. M., Voss, J., Mao, W. L., & Karunadasa, H. I. (2016). High-pressure single-crystal structures of 3D lead-halide hybrid perovskites and pressure effects on their electronic and optical properties. ACS central science, 2(4), 201-209.

(54) Schötz, K., Askar, A. M., Köhler, A., Shankar, K., & Panzer, F. (2020). Investigating the Tetragonal-to-Orthorhombic Phase Transition of Methylammonium Lead Iodide Single Crystals by Detailed Photoluminescence Analysis. Advanced Optical Materials, 8(17), 2000455.

(55) Kim, H. S., Lee, C. R., Im, J. H., Lee, K. B., Moehl, T., Marchioro, A., ... & Park, N. G. (2012). Lead iodide perovskite sensitized all-solid-state submicron thin

film mesoscopic solar cell with efficiency exceeding 9%. Scientific reports, 2(1), 591.

(56) Cao, J., Tai, Q., You, P., et al., 2019. Enhanced Performance of Tin-Based Perovskite Solar Cells Induced by an Ammonium Hypophosphite Additive. J. Mater. Chem. A 7, 26580–26585.

(57) Kopacic, I., Friesenbichler, B., Hoefler, S.F., et al., 2018. Enhanced Performance of Germanium Halide Perovskite Solar Cells through Compositional Engineering. ACS Appl. Energy Mater. 1, 343–347.

(58) Eckhardt, K., Bon, V., Getzschmann, J., Grothe, J., Wisser, F.M., Kaskel, S., 2016. Crystallographic Insights into (CH3NH3)3(Bi2I9): A New Lead-Free Hybrid Organic-Inorganic Material as a Potential Absorber for Photovoltaics. Chem. Commun. 52 (14), 3058–3060.

(59) Boopathi, K.M., Karuppuswamy, P., Singh, A., et al., 2017. Solution-Processable Antimony-Based Light-Absorbing Materials beyond Lead Halide Perovskites. J. Mater. Chem. A 5, 20843–20850.

(60) Ke, W., Stoumpos, C.C., Kanatzidis, M.G., 2018. “Unleaded” Perovskites: Status Quo and Future Prospects of Tin-Based Perovskite Solar Cells. Adv. Mater. 31, e1803230.

(61) Stoumpos, C.C., Malliakas, C.D., Kanatzidis, M.G., 2013. Semiconducting Tin and Lead Iodide Perovskites with Organic Cations: Phase Transitions, High Mobilities, and Near-Infrared Photoluminescent Properties. Inorg. Chem. 52, 9019–9038.

(62) Noel, N.K., Stranks, S.D., Abate, A., et al., 2014. Lead-Free Organic-Inorganic Tin Halide Perovskites for Photovoltaic Applications. Energy Environ. Sci. 7, 3061–3068.

(63) Hao, F., Stoumpos, C.C., Cao, D.H., Chang, R.P.H., Kanatzidis, M.G., 2014. LeadFree Solid-State Organic-Inorganic Halide Perovskite Solar Cells. Nat. Photonics 8 (6), 489–494.

(64) Green, M. A., Ho-Baillie, A., & Snaith, H. J. (2014). The emergence of perovskite solar cells. Nature photonics, 8(7), 506-514.

(65) Zhao, Z., Gu, F., Li, Y., Sun, W., Ye, S., Rao, H., ... & Huang, C. (2017). Mixed-organic-cation tin iodide for lead-free perovskite solar cells with an efficiency of 8.12%. Advanced Science, 4(11), 1700204.

(66) Wang, F., Ma, J., Xie, F., Li, L., Chen, J., Fan, J., & Zhao, N. (2016). Organic cation-dependent degradation mechanism of organotin halide perovskites. Advanced Functional Materials, 26(20), 3417-3423.

(67) Fujihara, T., Terakawa, S., Matsushima, T., Qin, C., Yahiro, M., & Adachi, C. (2017). Fabrication of high coverage MASnI 3 perovskite films for stable, planar heterojunction solar cells. Journal of Materials Chemistry C, 5(5), 1121-1127.

(68) Ke, W., Stoumpos, C. C., Spanopoulos, I., Mao, L., Chen, M., Wasielewski, M. R., & Kanatzidis, M. G. (2017). Efficient lead-free solar cells based on hollow {en} MASnI3 perovskites. Journal of the American Chemical Society, 139(41), 14800-14806.

(69) Zhu, Z., Chueh, C. C., Li, N., Mao, C., & Jen, A. K. Y. (2018). Realizing efficient lead-free formamidinium tin triiodide perovskite solar cells via a sequential deposition route. Advanced materials, 30(6), 1703800.

(70) Yang, Z., Zhong, M., Liang, Y., Yang, L., Liu, X., Li, Q., ... & Xu, D. (2019). SnO2-C60 Pyrrolidine Tris-Acid (CPTA) as the Electron Transport Layer for Highly Efficient and Stable Planar Sn-Based Perovskite Solar Cells. Advanced Functional Materials, 29(42), 1903621.

(71) Jiang, X., Li, H., Zhou, Q., Wei, Q., Wei, M., Jiang, L., ... & Ning, Z. (2021). One-step synthesis of SnI2·(DMSO) x adducts for high-performance tin perovskite solar cells. Journal of the American Chemical Society, 143(29), 10970-10976.

(72) Singh, A. K., Srivastava, S., Mahapatra, A., Baral, J. K., & Pradhan, B. (2021). Performance optimization of lead free-MASnI3 based solar cell with 27% efficiency by numerical simulation. Optical Materials, 117, 111193.

(73) Ke, W., Stoumpos, C.C., Logsdon, J.L., et al., 2016. TiO2–ZnS Cascade Electron Transport Layer for Efficient Formamidinium Tin Iodide Perovskite Solar Cells. J. Am. Chem. Soc. 138, 14998–15003.

(74) Ke, W., Stoumpos, C.C., Spanopoulos, I., et al., 2017. Efficient Lead-Free Solar Cells Based on Hollow {en}MASnI3 Perovskites. J. Am. Chem. Soc. 139, 14800–14806.

(75) Jokar, E., Chien, C.H., Tsai, C.M., et al., 2018. Robust Tin-Based Perovskite Solar Cells with Hybrid Organic Cations to Attain Efficiency Approaching 10%. Adv. Mater. 31, 1804835.

(76) D. Liu, Q. Li, H. Jing, K. Wu, Pressure-induced effects in the inorganic halide perovskite CsGeI3, RSC Adv. 9 (2019) 3279

(77) X. Wu, W. Song, Q. Li, X. Zhao, D. He, Z. Quan, Synthesis of lead-free CsGeI3 perovskite colloidal nanocrystals and electron beam-induced transformations, Chem. Asian J. 13 (2018) 1654–1659

(78) I. Kopacic, B. Friesenbichler, S.F. Hoelfer, B. Kunert, H. Plank, T. Rath, G. Trimmel, Enhanced performance of germanium halide perovskite solar cells through compositional engineering, ACS Appl. Energy Mater. 1 (2018) 343–347,

(79) A. Raj, M. Kumar, H. Bherwani, A. Gupta, A. Anshul, Evidence of improved power conversion efficiency in lead-free CsGeI3 based perovskite solar cell heterostructure via SCAPS simulation, J. Vac. Sci. Technol. B 39 (2021), 012401.

(80) A. Raj, M. Kumar, P.K. Singh, R.C. Singh, H. Bherwani, A. Gupta, A. Anshul, A computational approach to investigate the suitable ETL for lead-free CsGeI3 based perovskite solar cell, Mater. Today: Proc., DOI: 10.1016/j. matpr.2021.03.610

(81) T. Krishnamoorthy, H. Ding, C. Yan, W.L. Leong, T. Baikie, Z. Zhang, M. Sherburne, S. Li, M. Asta, N. Mathews, S.G. Mhaisalkar, Lead-free germanium iodide perovskite materials for photovoltaic applications, J. Mater. Chem. 3 (2015) 23829–23832.

(82) L.J. Chen, Synthesis and optical properties of lead-free cesium germanium halide perovskite quantum rods, RSC Adv. 8 (2018) 18396–18399.

(83) Sima, C, Grigoriu, C & Antohe, S 2010, 'Comparison of the dye-sensitized solar cells performances based on transparent conductive ITO and FTO', Thin Solid Films, vol. 519, no. 2, pp. 595-597.

(84) Tonui, P, Oseni, SO, Sharma, G, Yan, Q & Tessema Mola, G 2018, 'Perovskites photovoltaic solar cells: An overview of current status', Renewable and Sustainable Energy Reviews, vol. 91, pp. 1025-1044.

(85) Brenes, R, Guo, D, Osherov, A, Noel, NK, Eames, C, Hutter, EM, Pathak, SK, Niroui, F, Friend, RH & Islam, MS 2017, 'Metal halide perovskite polycrystalline films exhibiting properties of single crystals', Joule, vol. 1, no. 1, pp. 155-167.

(86) Lee, MM, Teuscher, J, Miyasaka, T, Murakami, TN & Snaith, HJ 2012, 'Efficient hybrid solar cells based on meso-super structured organometal halide perovskites', Science, vol. 338, no. 6107, pp. 643-647

(87) Bakr, ZH, Wali, Q, Fakharuddin, A, Schmidt-Mende, L, Brown, TM & Jose, R 2017, 'Advances in hole transport materials engineering for stable and efficient perovskite solar cells', Nano Energy, vol. 34, pp. 271-305.

(88) Adhikari, N., Dubey, A., Khatiwada, D., Mitul, A. F., Wang, Q., Venkatesan, S., ... & Qiao, Q. (2015). Interfacial study to suppress charge carrier recombination for high efficiency perovskite solar cells. ACS applied materials & interfaces, 7(48), 26445-26454.

(89) Rong, X, Tian, H, Bi, W, Jin, H, Zhang, T, Guo, D & Zhao, K 2017, 'Impact of metal electrode work function of CH3NH3PbI3/p-Si planar heterojunction perovskite solar cells', Solar Energy, vol. 158, pp. 424-431.

(90) Xie, X, Liu, G, Xu, C, Li, S, Liu, Z & Lee, E-C 2017, 'Tuning the work function of indium-tin-oxide electrodes for low-temperature-processed, titanium-oxide-free perovskite solar cells', Organic Electronics, vol. 44, pp. 120-125.

(91) Murakami, Takurou N., Seigo Ito, Qing Wang, Md Khaja Nazeeruddin, Takeru Bessho, Ilkay Cesar, Paul Liska et al. "Highly efficient dye-sensitized solar cells based on carbon black counter electrodes." Journal of the Electrochemical Society 153, no. 12 (2006): A2255.

(92) Veerappan, Ganapathy, Karunagaran Bojan, and Shi-Woo Rhee. "Sub-micrometer-sized graphite as a conducting and catalytic counter electrode for dye-sensitized solar cells." ACS applied materials & interfaces 3, no. 3 (2011): 857-862.

(93) Li, Yu-Yan, Chun-Ting Li, Min-Hsin Yeh, Kuan-Chieh Huang, Ping- Wei Chen, R. Vittal, and Kuo-Chuan Ho. "Graphite with different structures as catalysts for counter electrodes in dye-sensitized solar cells." Electrochimica Acta 179 (2015): 211-219.

(94) Imoto, Kiyoaki, Kohshin Takahashi, Takahiro Yamaguchi, Teruhisa Komura, Jun-ichi Nakamura, and Kazuhiko Murata. "High- performance carbon counter electrode for dye-sensitized solar cells." Solar Energy Materials and Solar Cells 79, no. 4 (2003): 459-469.

(95) Wei, Wei, Hui Wang, and Yun Hang Hu. "A review on PEDOT-based counter electrodes for dye-sensitized solar cells." International Journal of Energy Research 38, no. 9 (2014): 1099-1111.

(96) Yella, A., Lee, H.W., Tsao, H.N., Yi, C., Chandiran, A.K., Nazeeruddin, M.K., Diau, E.W.G., Yeh, C.Y., Zakeeruddin, S.M. and Grätzel, M. (2011) 'Porphyrin-

sensitized solar cells with cobalt (II/III)–based redox electrolyte exceed 12 percent efficiency', Science, 334(6056), pp.629-634.

(97) Hersch, P. and Zweibel, K. (1982) Basic photovoltaic principles and methods (No. SERI/SP-290-1448), Solar Energy Research Institute, Golden, CO (USA).

(98) Kim, H. S., Lee, C. R., Im, J. H., Lee, K. B., Moehl, T., Marchioro, A. and Grätzel, M. (2012) 'Lead iodide perovskite sensitized all-solid-state submicron thin film mesoscopic solar cell with efficiency exceeding 9%' Scientific Reports, 2, pp.591(1-7).

(99) A.Marchioro, J. Teuscher, D. Friedrich et al., "Unravelling the mechanism of photoinduced charge transfer processes in lead iodide perovskite solar cells," Nature Photonics, vol. 8, no. 3, pp. 250–255, 2014.

This Page is intentionally left blank